Electronic Supplementary Information

Charge-order driven proton arrangement in a hydrogen-bonded charge-transfer complex based on a pyridyl-substituted TTF derivative

Sang Chul Lee,*[a] Akira Ueda,*[a] Hiromichi Kamo,[a] Kazuyuki Takahashi,[b] Mikio Uruichi,[c] Kaoru Yamamoto,[c] Kyuya Yakushi,[c] Akiko Nakao,[d] Reiji Kumai,[e] Kensuke Kobayashi,[e] Hironori Nakao,[e] Youichi Murakami[e] and Hatsumi Mori*[a]

[a] *The Institute for Solid State Physics, The University of Tokyo, 5-1-5 Kashiwanoha, Kashiwa, Chiba, 277-8581, Japan. Tel/Fax: +81-4-7136-3410; E-mail: hmori@issp.u-tokyo.ac.jp*

[b] *Department of Chemistry, Graduate School of Science, Kobe University, Kobe, Hyogo 657–8501, Japan*

[c] *Institute for Molecular Science, Okazaki, Aichi 444–8585, Japan*

[d] *Research Center for Neutron Science and Technology, CROSS, Tokai–mura, Ibaraki 319–1106, Japan*

[e] *Condensed Matter Research Center, Institute of Materials Structure Science, KEK, Tsukuba, Ibaraki 305–0801, Japan*

General Information

Py-TTF and Li·F_4TCNQ were prepared according to the literatures.[S1,S2] Other commercially available materials were used as received. Elemental analyses of C, H, and N were performed using a CE-440 CHN/O/S elemental analyzer. Cyclic voltammetry (CV) experiments were performed on a YANACO P1100 polarographic analyzer in MeCN solution containing 0.1 M Bu_4NClO_4 (working electrode: Pt, counter electrode: Pt wire, reference electrode: saturated calomel electrode (SCE)). IR spectra were recorded using KBr pellets on a Horiba FT-730 infrared spectrometer. UV-vis spectra were recorded using CH_3CN solution on a Hitachi UV-3010 UV-vis spectrometer. X-ray crystallographic measurements were made on the diffractometer by synchrotron radiation with a Weissenberg-type imaging plate detector at BL-8A in the Photon Factory at KEK, Japan (λ = 1.0000 Å at 298 K) for $(PyH^{+}–TTF^{0.3+}Py–TTF^{0.7+})(F_4TCNQ^{\bullet-})_2$•MeCN, on a Rigaku AFC-7R diffractometer (Mo-Kα, λ = 0.71075 Å) for neutral Py-TTF and on a Rigaku CMF007 Mercury CCD (Mo-Kα, λ = 0.71069 Å) for $(PyH^{+}–TTF)(BF_4^{-})(H_2O)$, respectively. The direct current electrical conductivity measurement was made by the conventional four-probe method using carbon paste and gold wires. The transfer integrals and the band structures were calculated within the tight-binding approximation using the extended Hückel molecular orbital method.[S3] Molecular orbital and proton potential calculations were performed with: Frisch, M. J.; et al. *Gaussian 03*, revision E.01; Gaussian Inc.: Wallingford CT, 2004.[S4]

Preparation of materials

• Neutral Py-TTF donor:

Py-TTF was prepared according to the literature.[S1] An orange plate crystal suitable for X-ray analysis was obtained by slow evaporation of hexane-CH_2Cl_2 solution at room temperature.

• Protonated BF_4 salt (PyH^+–TTF)(BF_4^-)(H_2O):

In a 200-mL Erlenmeyer flask, Py-TTF (100 mg, 0.258 mmol) was suspended in MeCN (10 mL). To the resulting orange suspension, a few drops of 54% HBF_4 in Et_2O were added, and then the suspension immediately changed to a dark violet solution. After addition of Et_2O (100 mL), the resulting solution was allowed to stand overnight at room temperature, to give the desired BF_4 salt (99.6 mg, 76%) as violet blockish crystals. mp 179-181 ºC; IR (KBr) 3190-2960, 2930-2390, 1634, 1558, 1534, 1507 cm^{-1}; Anal. Calcd for ($C_{11}H_8NS_4$)(BF_4)(H_2O): C, 34.12; H, 2.60; N, 3.62%. Found: C, 34.05; H, 2.81; N, 3.51%.

• H-bonded CT complex, (PyH^+–$TTF^{0.3+}$Py–$TTF^{0.7+}$)($F_4TCNQ^{\bullet-}$)$_2$•MeCN:

In a 100-mL Erlenmeyer flask, a suspension of Li·F_4TCNQ (17.1 mg, 0.06 mmol) in MeCN (50 mL) was boiled at 82 ºC for a few minutes and then the suspension was filtered to remove insoluble matter. After cooling down to room temperature, the filtrate was transferred to a 200-mL Erlenmeyer flask. To the solution were added F_4TCNQ (16.5 mg, 0.06 mmol) in MeCN (50 mL) and the BF_4 salt of PyH^+-TTF (46.5 mg, 0.12 mmol) in MeCN (50 mL). The resulting mixture was shaken and then allowed to stand for overnight at room temperature, to give the CT complex (24.3 mg, 17%) as violet platelet crystals. mp 165 ºC (gradually decomposed); IR (KBr) 2800-1800 (originated from N^+-H…N type hydrogen bond), 2196, 2170, 1628, 1597, 1533, 1500, 1386, 1341 cm^{-1}; Anal. Calcd for ($C_{22}H_{15}N_2S_8$)($C_{12}F_4N_4$)$_2$(MeCN): Calcd (%): C, 49.82; H, 1.57; N,13.31. Found (%): C, 49.57; H, 1.23; N, 12.95.

Table S1. Crystallographic data of Py-TTF, $(PyH^{+}–TTF)(BF_4^{-})(H_2O)$, and $(PyH^{+}–TTF^{0.3+}Py–TTF^{0.7+})(F_4TCNQ^{\bullet-})_2$•MeCN.

	Py-TTF	$(PyH^{+}–TTF)(BF_4^{-})(H_2O)$	$(PyH^{+}–TTF^{0.3+}Py–TTF^{0.7+})(F_4TCNQ^{\bullet-})_2$•MeCN
Formula	$C_{11}H_7N_1S_4$	$C_{11}H_{10}B_1N_1O_1F_4S_4$	$C_{48}H_{18}N_{11}S_8F_8$
Crystal System	orthorhombic	triclinic	monoclinic
Space Group	$P2_12_12_1$ (#19)	P-1 (#2)	$P2_1/n$ (#14)
a / Å	3.971(3)	6.801(4)	22.0041(4)
b / Å	11.487(9)	7.939(5)	7.0211(4)
c / Å	25.41(2)	14.424(8)	31.0684(7)
α / °	90	90.83(2)	90
β / °	90	96.20(3)	95.8755(7)
γ / °	90	92.08(2)	90
V / Å^3	1159(2)	733.6(8)	4774.6(3)
Z value	4	2	4
Temperature / K	293	293	293
d_{calc} / g·cm^{-3}	1.613	1.654	1.610
λ / Å	0.71073	0.71070	1.0000
# of observations	1448	3462	10840
# of variables	152	200	680
R_1 ($I > 2.0\sigma(I)$)	0.0610	0.0790	0.0436
wR_2 (all data)	0.1077	0.2171	0.1438
GOF	1.006	1.243	0.967
CCDC number	887353	887354	887352

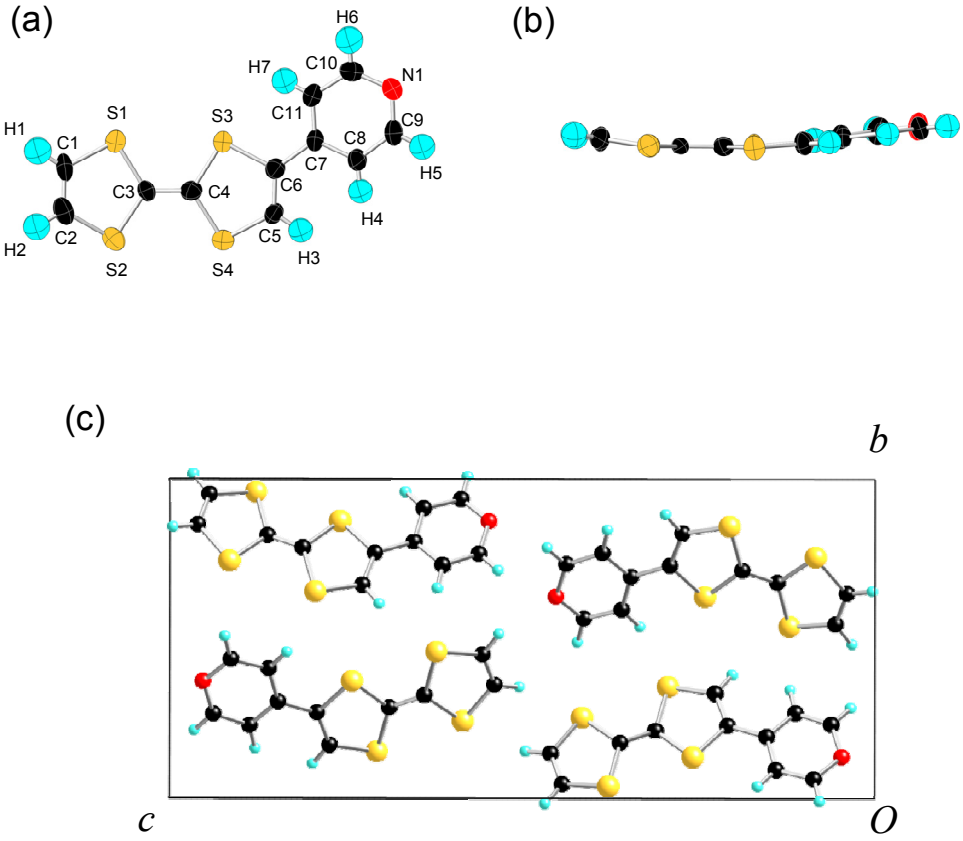

Figure S1. X-ray crystal structure of the neutral Py-TTF: (a) top view, (b) side view and (c) crystal packing viewed along the *a*-axis.

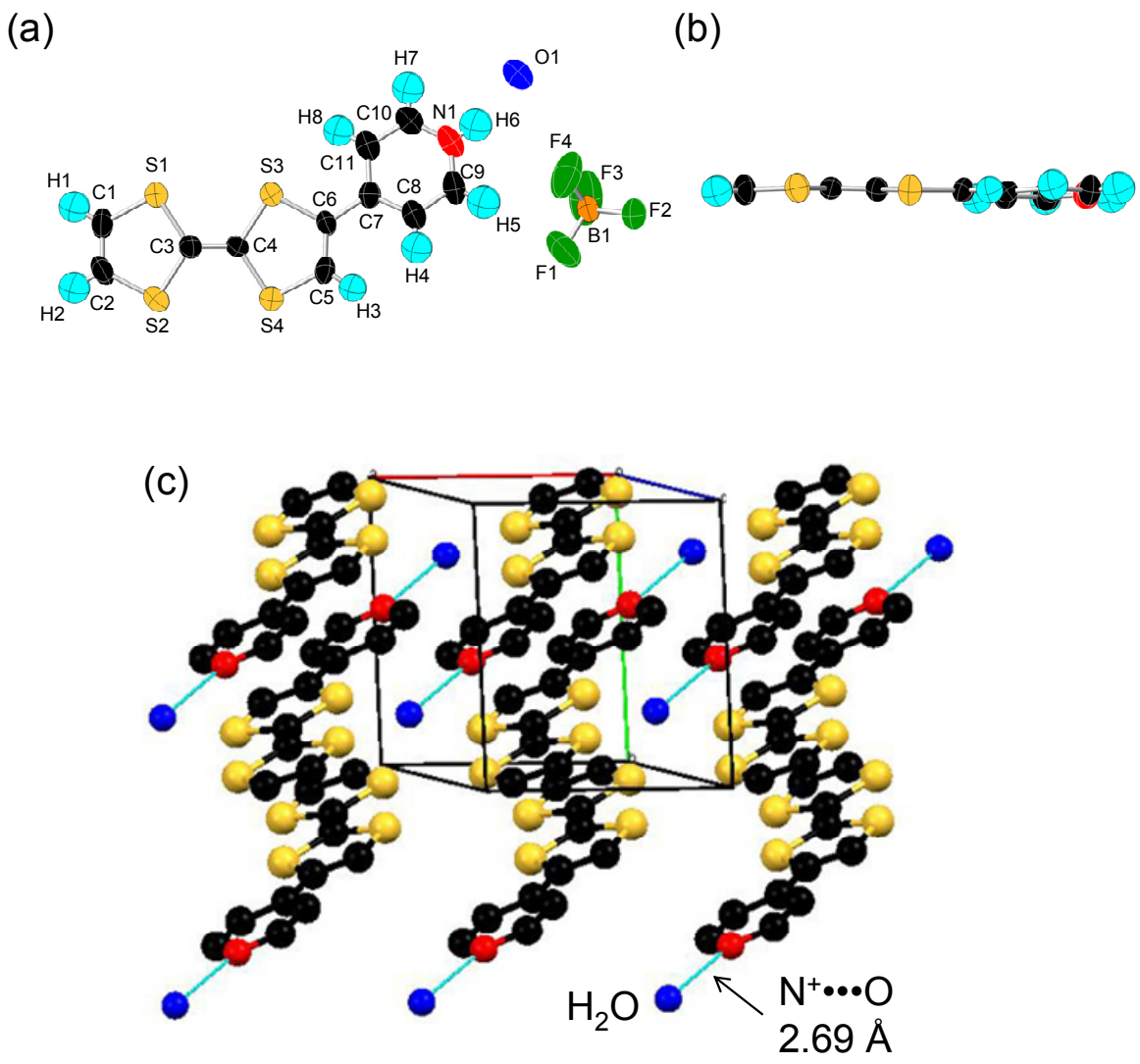

Figure S2. X-ray crystal structure of (PyH^+-TTF)(BF_4^-)(H_2O): (a) top and (b) side views of PyH^+-TTF and (c) packing structure with N^+–H•••O H-bonds between PyH^+-TTF and H_2O. In (c), hydrogen atoms and BF_4^- anion were omitted for clarity.

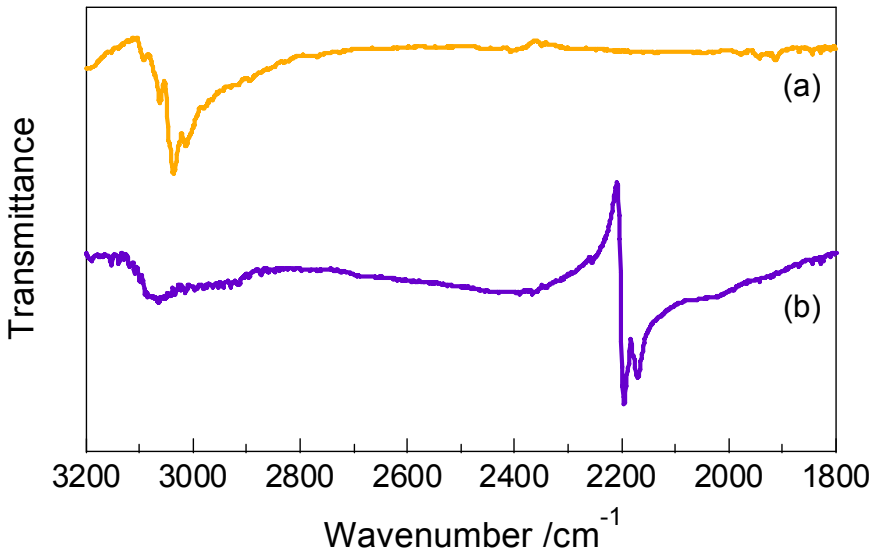

Figure S3. IR spectra of (a) neutral Py-TTF and (b) the CT complex in KBr pellet. A broad absorption band at 1800-2800 cm^{-1} in (b) is probably attributable to the NH stretching in an N^{+}–H•••N type H-bond.

Table S2. Comparison of the C-N-C bond angle of the pyridine ring in the neutral Py-TTF, the protonated PyH^+-TTF salt, and the donors **A** and **B** in the CT complex. Similar to the literature,[S5] the pyridine C-N-C bond angle of this system becomes larger by protonation (the neutral Py-TTF (115.4°) and the protonated PyH^+-TTF (121.9°)). Interestingly, the value of the protonated donor **A** (121.5°) is slightly smaller than that of the fully protonated PyH^+-TTF (121.9°) and the value of the non-protonated donor **B** (117.2°) is also slightly larger than that of the completely neutral Py-TTF (115.4°). This result indicates that the donors **A** and **B** are not completely protonated or non-protonated, reflecting the N^+–H•••N type hydrogen-bond formation between the donors **A** and **B**.

	C-N-C bond angle / °
neutral Py-TTF	115.4
PyH^+-TTF BF_4 salt	121.9
donor **A** (protonated)	121.5
donor **B** (non-protonated)	117.2

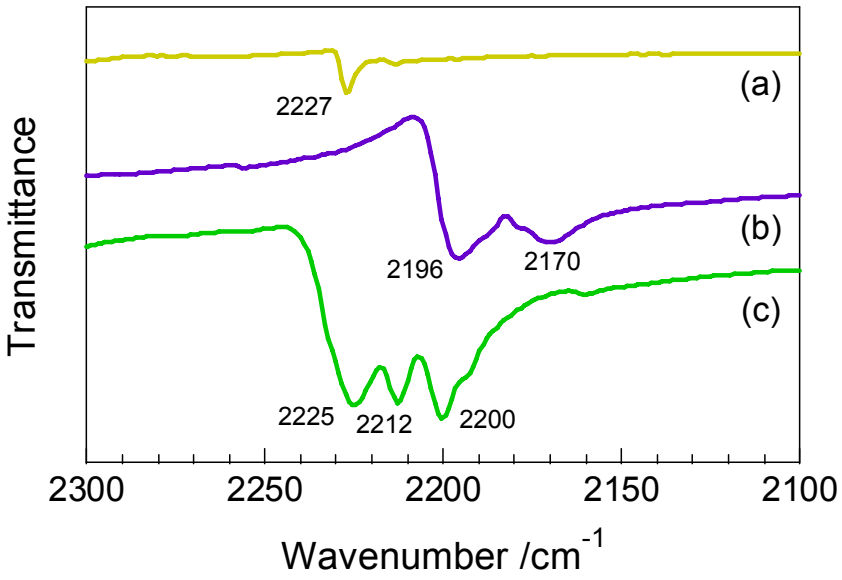

Figure S4. The CN stretching modes in IR spectra of (a) neutral F_4TCNQ, (b) the CT complex and (c) Li·F_4TCNQ in KBr pellet.

Table S3. Comparison of bond lengths of the acceptors **C** and **D** in the CT complex, neutral F_4TCNQ[S6] and F_4TCNQ radical anion[S7].

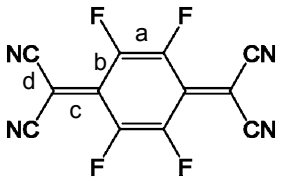

	a / Å	b / Å	c / Å	d / Å
F_4TCNQ^0 [S6]	1.334	1.436	1.372	1.435
Acceptor **C**	1.358(4)	1.418(4)	1.412(4)	1.420(5)
Acceptor **D**	1.344(4)	1.414(4)	1.402(4)	1.426(4)
TBA•$F_4TCNQ^{\bullet -}$ [S7]	1.357	1.415	1.418	1.425

Table S4. Charge estimation of the TTF moiety of the donors **A** and **B** by bond length analysis. The bond length of **a** for **A** (1.357(3) Å) and **B** (1.380(3) Å) is intermediated between that of the neutral Py-TTF (1.344(9) Å) and the TTF radical cation (1.393 Å)[S8], suggesting that A and B are partially oxidized. Each tentative charge δ_1^+ obtained by the literature's equation[S9] was corrected by considering the substitution effect of the pyridyl or pyridinium group, to give δ_2^+ of +0.415 (= +0.305 – (–0.110)) for the protonated **A** and δ_2^+ of +0.974 (= +0.903 – (–0.071)) for the non-protonated **B**. Finally their real charge δ_3^+ was estimated to +0.3 for **A** and +0.7 for **B** by normalization of the δ_2^+ values (i.e., sum of the two δ_2^+ value was set to +1).

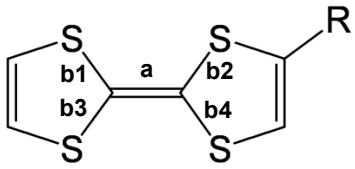

$$(\mathbf{b1}+\mathbf{b2}+\mathbf{b3}+\mathbf{b4})/4 = 1.757 - 0.0385\delta_1^+$$

	a / Å	**b1** / Å, **b2** / Å **b3** / Å, **b4** / Å	δ_1^+	δ_2^+	δ_3^+
Donor **A** (protonated)	1.357(3)	1.743(3), 1.749(3) 1.742(3), 1.747(3)	+0.305	+0.415 (= +0.305 – (–0.110))	+0.298 (= +0.415/(+0.415+0.974))
Donor **B** (non-protonated)	1.380(3)	1.714(3), 1.729(3) 1.727(4), 1.719(3)	+0.903	+0.974 (= +0.903 – (–0.071))	+0.701 (= +0.974/(+0.415+0.974))
Py-TTF^0	1.344(9)	1.762(7), 1.755(7) 1.756(6), 1.766(7)	–0.071		
(PyH$^+$-TTF)(BF_4^-)(H_2O)	1.331(7)	1.755(5), 1.765(5) 1.763(5), 1.762(5)	–0.110		
$TTF^{\bullet+}$ Br [S8]	1.393	1.720	+0.987		

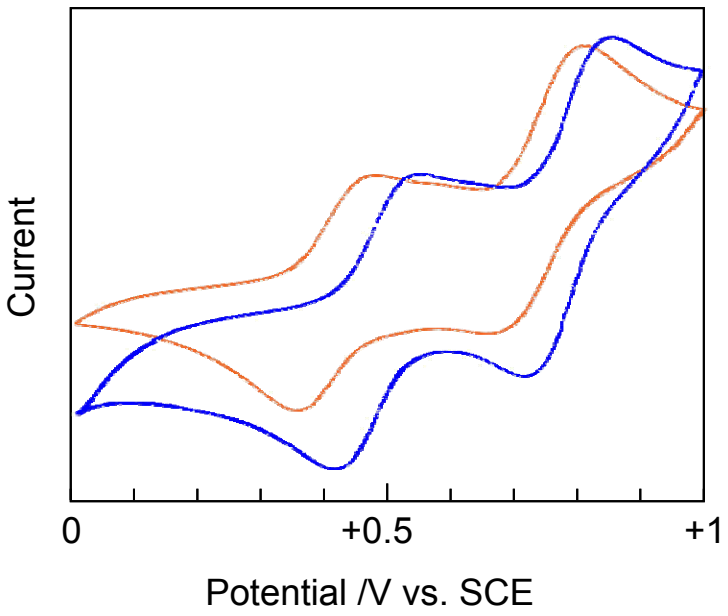

Figure S5. Cyclic voltammograms of Py-TTF (orange line) and PyH^+-TTF (blue line, protonated by addition of an excess amount of *p*-toluenesulfonic acid) in 10 mM MeCN solution containing 0.1 M Bu_4NClO_4 (working electrode: Pt, counter electrode: Pt wire, reference electrode: saturated calomel electrode (SCE)).

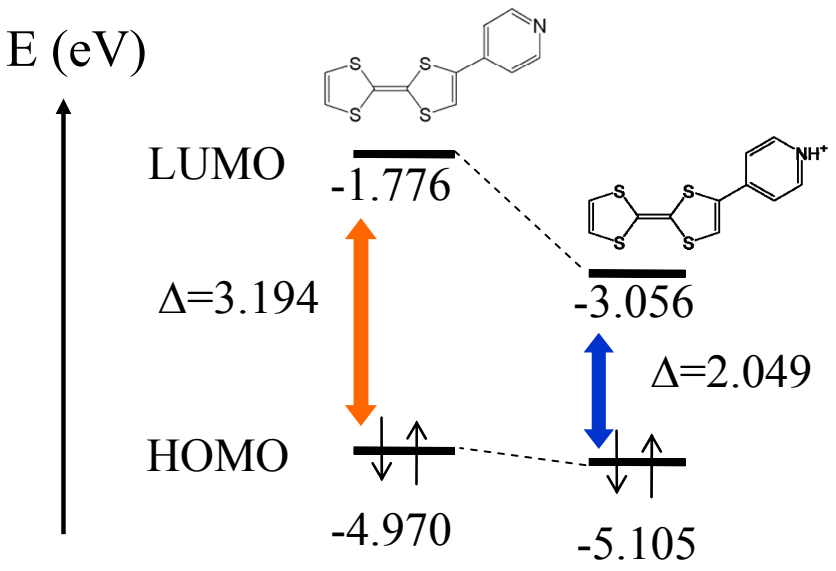

Figure S6. Energy diagram of Py-TTF and PyH^{+}-TTF calculated by GAUSSIAN 03 at the PCN (MeCN)/B3LYP/6-311G** level of theory.

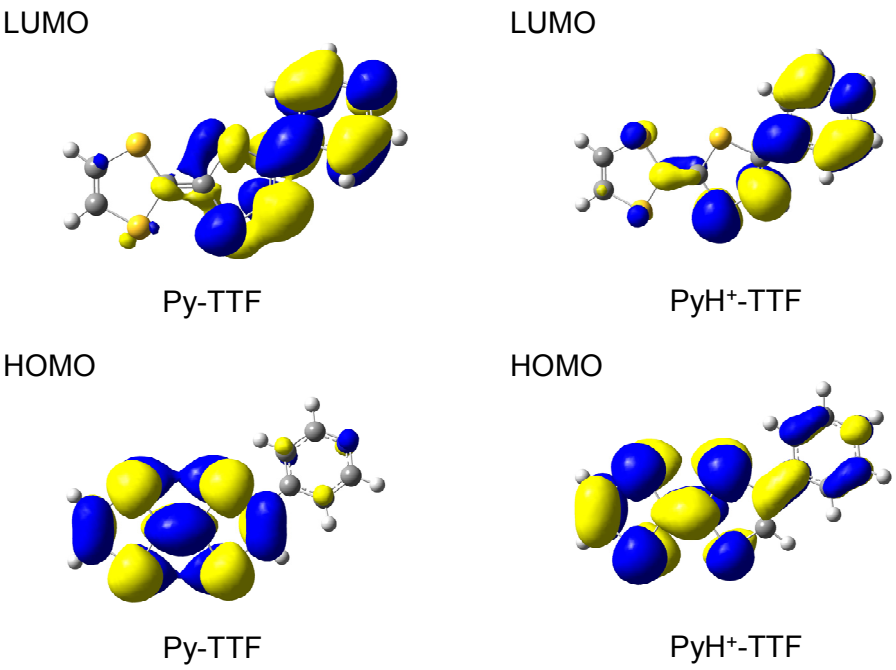

Figure S7. HOMO and LUMO distribution maps of Py-TTF and PyH^+-TTF calculated by GAUSSIAN 03 at the B3LYP/6-311G** level of theory.

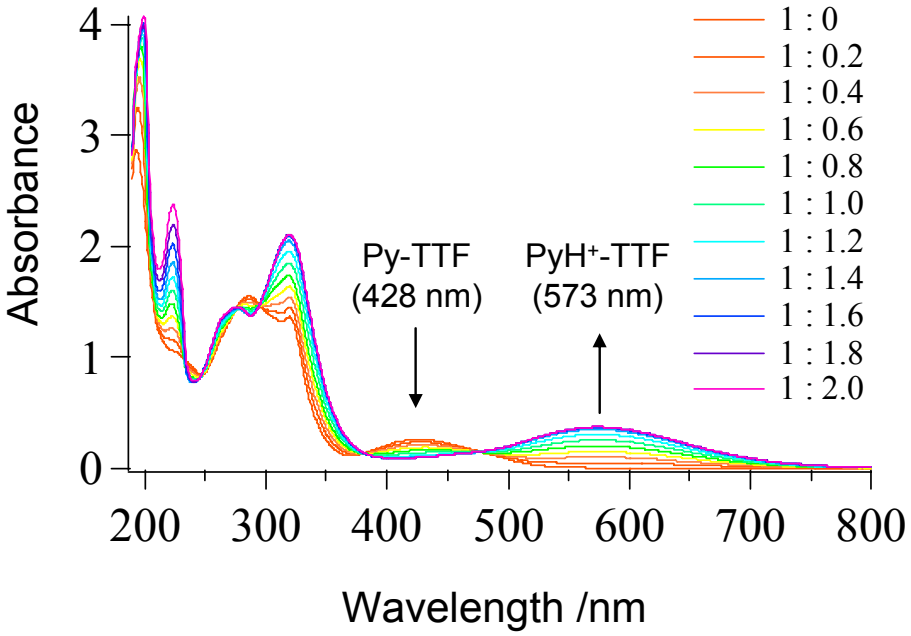

Figure S8. UV-vis spectrum change of Py-TTF in CH_3CN (10^{-4} M) with increasing concentration of *p*-toluenesufonic acid (molar ratio). Intramolecular charge transfer (ICT) band of PyH^+-TTF (573 nm) is significantly red-shifted compared to that of Py-TTF (428 nm), suggesting a much smaller HOMO-LUMO energy gap of PyH^+-TTF (see also Figure S6).

Table S5. Transfer integrals of the donors **A**, **B** in the CT complex calculated by extended Hückel method [S3] and the intermolecular donor distances (Symbols are shown in the figure below).

	t ×10^{-2} /eV	Distances / Å
a_1	-18.2	3.53 (inter-dimer)
a_2	-21.4	3.50 (intra-dimer)
b	2.7	3.74, 3.83 (S-S)
p_1	-1.1	5.20 (S-S)
p_2	-0.2	4.81, 4.91 (S-S)

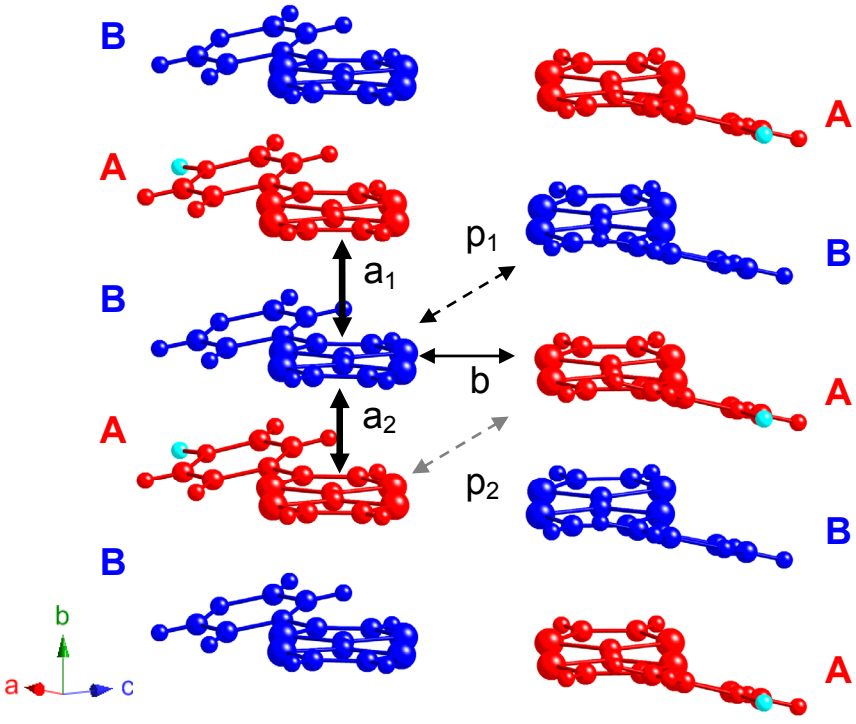

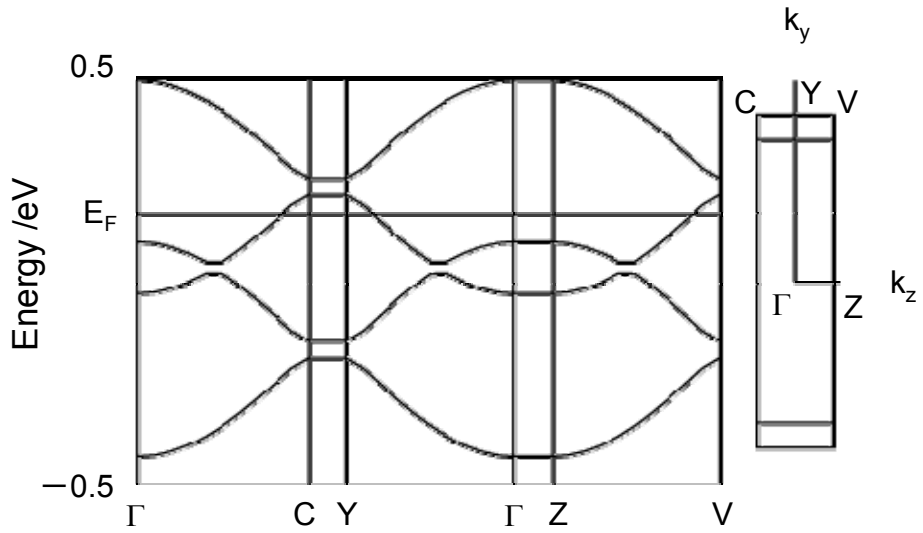

Figure S9. Energy dispersion and Fermi surface of the CT complex calculated by extended Hückel method with tight-binding approximation.[S3]

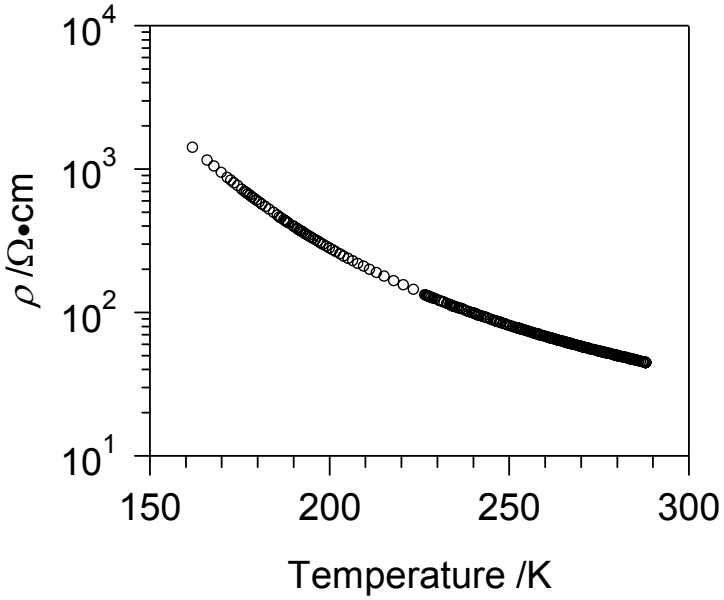

Figure S10. Temperature dependence of electrical resistivity of the H-bonded CT complex along the π-stacking direction (*b*-axis).

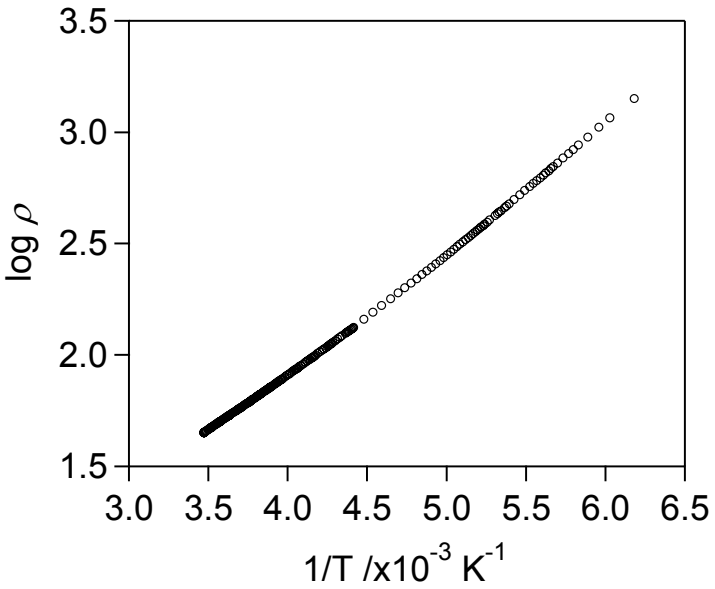

Figure S11. Arrhenius plot of the resistivity of the CT complex. Activation energy (0.12 eV) was calculated by the fitting of this plot under 200 K.

References

S1) L. Wang, B. Zhang and J. Zhang, *Inorg. Chem*., 2006, **45**, 6860.

S2) L. R. Melby, R. J. Harder, W. R. Hertler, W. Marler, R. E. Benson and W. E. Mochel, *J. Am. Chem. Soc.*, 1962**, 84**, 3374.

S3) T. Mori, A. Kobayashi, Y. Sasaki, H. Kobayashi, G. Saito and H. Inokuchi, *Bull. Chem. Soc. Jpn.*, 1984, **57**, 627.

S4) M. J. Frisch, G. W. Trucks, H. B. Schlegel, G. E. Scuseria, M. A. Robb, J. R. Cheeseman, J. A. Montgomery, Jr., T. Vreven, K. N. Kudin, J. C. Burant, J. M. Millam, S. S. Iyengar, J. Tomasi, V. Barone, B. Mennucci, M. Cossi, G. Scalmani, N. Rega, G. A. Petersson, H. Nakatsuji, M. Hada, M. Ehara, K. Toyota, R. Fukuda, J. Hasegawa, M. Ishida, T. Nakajima, Y. Honda, O. Kitao, H. Nakai, M. Klene, X. Li, J. E. Knox, H. P. Hratchian, J. B. Cross, V. Bakken, C. Adamo, J. Jaramillo, R. Gomperts, R. E. Stratmann, O. Yazyev, A. J. Austin, R. Cammi, C. Pomelli, J. W. Ochterski, P. Y. Ayala, K. Morokuma, G. A. Voth, P. Salvador, J. J. Dannenberg, V. G. Zakrzewski, S. Dapprich, A. D. Daniels, M. C. Strain, O. Farkas, D. K. Malick, A. D. Rabuck, K. Raghavachari, J. B. Foresman, J. V. Ortiz, Q. Cui, A. G. Baboul, S. Clifford, J. Cioslowski, B. B. Stefanov, G. Liu, A. Liashenko, P. Piskorz, I. Komaromi, R. L. Martin, D. J. Fox, T. Keith, M. A. Al-Laham, C. Y. Peng, A. Nanayakkara, M. Challacombe, P. M. W. Gill, B. Johnson, W. Chen, M. W. Wong, C. Gonzalez and J. A. Pople, *GAUSSIAN 03 (Revision E.01)*, Gaussian, Inc., Wallingford CT, 2004.

S5) T. Steiner, *Angew. Chem. Int. Ed*. 2002, **41**, 48.

S6) T. J. Emge, W. A. Bryden, F. M. Wiygul, D. O. Cowan and T. J. Kistenmacher, *J. Chem. Phys.* 1982*,* **77**, 3188.

S7) S. A. O'Kane, R. Clerac, H. Zhao, X. Ouyang, J. R. Galan-Mascaros, R. Heintz and K. R. Dunbar, *J. Solid State Chem.*, 2000, **152**, 159.

S8) R. C. Teitelbaum, T. J. Marks and C. K. Johnson, *J. Am. Chem. Soc.* 1980**, 102**, 2986.

S9) D. A. Clemente and A. Marzotto, *J. Mater. Chem*., 1996, **6**, 941.